

AD-A193 396

SOLAR FLARES AND MAGNETOSPHERIC PARTICLES

1/1

INVESTIGATIONS BASED UPON THE (U) LOUISIANA STATE UNIV

BATON ROUGE DEPT OF PHYSICS AND ASTRONOM

J P WEFEL

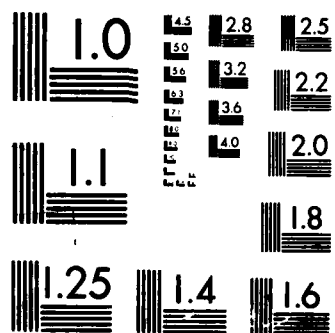
UNCLASSIFIED

10 FEB 88 N00014-83-K-0165

F/G 3/2

NL





AD-A193 396

ANNUAL LETTER REPORT

ONR Contract N00014-83-K-0365

"Solar Flares and Magnetospheric Particles:

Investigations Based Upon the ONR-602 and ONR-604 Experiments"

DTIC
ELECTE
APR 05 1988
S D

John P. Wefel

Principal Investigator

For the Period Ending: 30 November 1987

DISTRIBUTION STATEMENT A

Approved for public release
Distribution Unlimited

Louisiana State University
Department of Physics and Astronomy
Baton Rouge, LA 70803-4001

10 February 1988

88 3 001

SUMMARY

A-1

"SOLAR FLARES AND MAGNETOSPHERIC PARTICLES:
INVESTIGATIONS BASED UPON THE ONR-602 AND THE ONR-604 EXPERIMENTS"
ONR Contract N00014-83-K-0365

Annual Letter Report

I. INTRODUCTION:

This report covers the period to 30 November 1987 for the contract cited above. The research consists of fundamental investigations of the charged particle component in the Geospace environment. The project involves analysis of the data returned from the ONR-602 (Phoenix-1) experiment on the S81-1 mission in 1982, correlation of the Phoenix-1 dataset with other measurements, modeling the processes and the environment to understand the data, and scientific planning for the launch and operation of a "sister experiment," ONR-604 on the CRRES mission. During the past year significant progress has been made in interpreting the ONR-602 dataset with respect to the low-energy protons observed in the equatorial belt and the solar energetic particle observations.

II. Personnel:

The personnel engaged in this analysis effort consist of the principal investigator; one graduate student, Mr. M. A. Miah, working full-time on the project; a Senior Research Associate, Dr. T. G. Guzik working part-time on the analysis; a Research Associate, Dr. J. W. Mitchell who works part-time on the interpretation and modeling; and several undergraduate students to help with programming and data handling. In the coming year we expect to have Dr. John Cooper join the group. Dr. Cooper is an expert on magnetospheres and their interactions, and has worked previously with particle data measured in the magnetospheres of Saturn and Uranus. His experience and insight will be invaluable for both the ONR-602 analysis and the CRRES data.

III. Facilities:

The majority of the ONR-602 data analysis is now handled on the Experimental Physics Data System (EPDS), a VAX-11/750 based system containing 450 Mbytes of disk, three tape drives, a line printer and a Calcomp plotter as peripherals. The EPDS replaced a small PDP-11/73 and has improved both our data handling/analysis capabilities and our compatibility with the data systems at other facilities with which we work, e.g. University of Chicago, Naval Research Laboratory, etc.

During this program period we have been successful in obtaining "node status" on SPAN (Space Physics Analysis Network) and have installed the needed hardware and software. This national network provides access, from the EPDS, to most other space physics facilities in the country, including the NSSDC at Goddard, MSFC, University of Chicago, and, through ARPANET, the Aerospace Corporation and AFGL. This speeds communications with collaborators, provides for data transfer, and will be invaluable for working the CRRES program, both pre-launch and post-launch. We are currently gaining experience with the network and its impact on the resources of the EPDS system and our interpretive/modeling effort.

IV. PUBLICATIONS, REPORTS AND PRESENTATIONS:

A. Solar Energetic Particles and Galactic Cosmic Rays

1. Dr. T. Gregory Guzik of our group was invited to write a review paper on solar energetic particles. This has been completed and reviewed by three outside reviewers. Their comments were very helpful and led to a reworking of several sections of the paper. This manuscript, "The SEP Matter Sample and its Correlation with Gamma Ray Observations" has now been accepted for publication in Solar Physics during 1988.

2. Dr. John P. Wefel wrote an invited review paper entitled "An Overview of Cosmic Ray Research: Composition, Acceleration and Propagation." This paper details the connections between galactic cosmic rays and solar energetic particles and the physical processes occurring on the sun and elsewhere in the galaxy. The paper was just published in the NATO ASI Series C, Vol. 220, Mathematical and Physical Sciences (D. Reidel and Co., Dordrecht, Holland, 1988) p. 1-40.

B. International School for Space Simulation (ISSS-3)

Mr. M. Adel Miah was awarded a NASA fellowship to attend the ISSS-3 course in France during June 1987. With some additional financial aid from the French, he was able to attend both parts of the ISSS-3 meeting thereby gaining valuable experience in the computer simulation/modeling of the magnetospheric environment and by participating in the scientific program. He contributed a poster presentation about our work which drew the attention of Dr. T. Eastman from NASA who pointed out the need for such measurements in planning programs in LEO, such as the space station.

C. Chapman Conference

This past year's Chapman Conference was held in Sendai, Japan, October 12-16, 1987 and was devoted to "Plasma Waves and Instabilities in Magnetospheres and at Comets." Mr. M. Adel Miah received an NSF scholarship to attend this conference and present a paper. A copy of the abstract is attached. This paper has been prepared for publication in the Journal of Geophysical Research, and should appear in late 1988.

D. NATO ASI

A lecture describing our work was presented at the NATO ASI in Erice, Sicily, Italy in June, 1986. During the past year we have written this lecture for publication in the proceedings of that meeting. The paper was reviewed and accepted and has just appeared: "Phoenix-1 Observations of Equatorial Zone Particle Precipitation," M. A. Miah, T. G. Guzik, J. W. Mitchell and J. P. Wefel, in Genesis and Propagation of Cosmic Rays, eds. M. M. Shapiro and J. P. Wefel, (Dordrecht, Holland, 1988, D. Reidel and Co.), NATO ASI Series C, Vol. 220, p. 339-355.

V. RESEARCH HIGHLIGHTS:

One of the on-going problems in the interpretation of magnetospheric particle data is the determination of the intensity of non-isotropic, trapped particles. This problem arises because the particles are trapped in cyclotron orbits around magnetic field lines. Thus, at a particular altitude and longitude the trapped particle population is characterized by an equatorial pitch angle distribution to which different instruments will not have the same response. Therefore, measurement of absolute intensity is necessary to compare observations made by different instruments and/or over different time periods.

The motion of a charged particle trapped in the magnetosphere is a composite of a gyration around the field line on which it is trapped (cyclotron motion), a translation (bounce) along the field line and (for particles which remain trapped for long periods) a slow drift around the Earth. Neglecting the latter, the motion of the particle is helical and may be characterized at any point by its pitch angle (α), the angle between the velocity vector of the particle and field line. Since the motion of the particle at any point on the field line can be determined from its equatorial pitch angle (and the known field distribution), the overall trapped particle population can be represented by an equatorial distribution in pitch angle.

In the past year we have solved the problem of comparing our data to other observations by computing the telescope efficiency as a function of pitch angle. Figure 1 shows a schematic representation of the monitor telescope. Even though it consists of only a single detector, the passive shielding around the detector makes it a telescope characterized by a conical acceptance. A particle with an incident velocity vector within this cone will be seen by the telescope. For the central point on the detector, the acceptance cone is right circular while for off-center points the cone is skewed. This requires the calculation of telescope efficiency to be performed as a function of position on the surface of the detector. In order to simplify the process, the detector was divided into equal sub-areas, and (Figure 2 shows an example of the division of the detector area into 25 equal sub-areas), the central point of each being used to perform the calculation. For the final results, the detector was divided into 10^2 - 10^3 such sub-areas.

In order to determine the efficiency of the telescope for sampling the overall particle population at any point in space, we must know the pitch angle distribution at that point as well as the telescope efficiency as a function of pitch angle, taking into consideration the orientation of the telescope relative to the magnetic field. This calculation is facilitated by noting that all possible particle trajectories with pitch angle α which pass through a given point on the detector lie on the surface of a cone whose apex is at that point and whose half angle is α . The portion of the pitch angle cone which intercepts the telescope cone represents particle trajectories that will be seen by the telescope. The efficiency for a given pitch angle is, then, the fraction of the pitch angle cone over which particles can be observed. Mapping these cones onto one another involves putting the geomagnetic field vector and the telescope into the same coordinate system. The magnetic field vector can be transformed to the detector coordinate system for a given point on the orbit. This involves taking into account the latitude, the longitude, the altitude, the orbital inclination and (for a

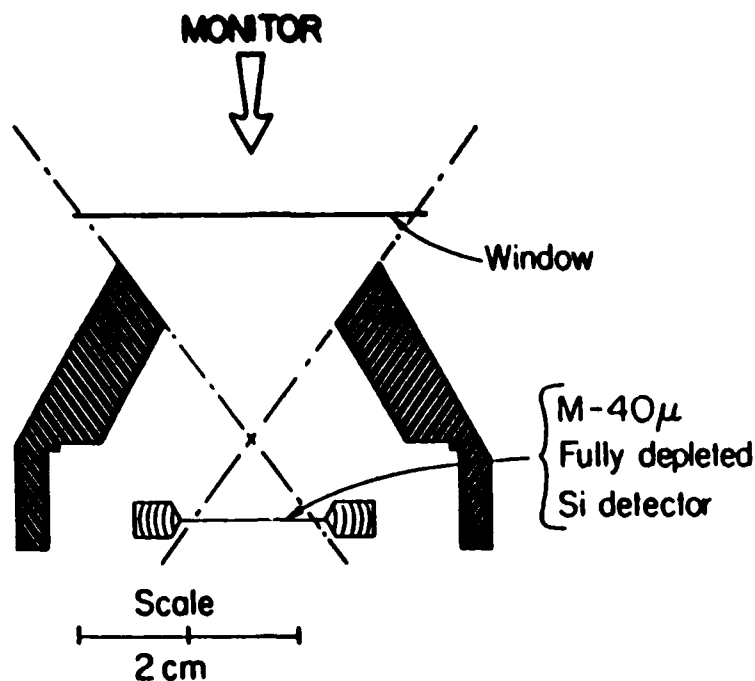


Figure 1. Geometry of the Monitor telescope used in the efficiency calculation. The full opening angle is 75° , the height of the telescope from the Si detector to the top of the window is 1.736 cm. Radius of the circular detector is 0.5639 cm, and the radius of the window is 0.776 cm. The shaded shielding stops protons up to ~ 40 MeV.

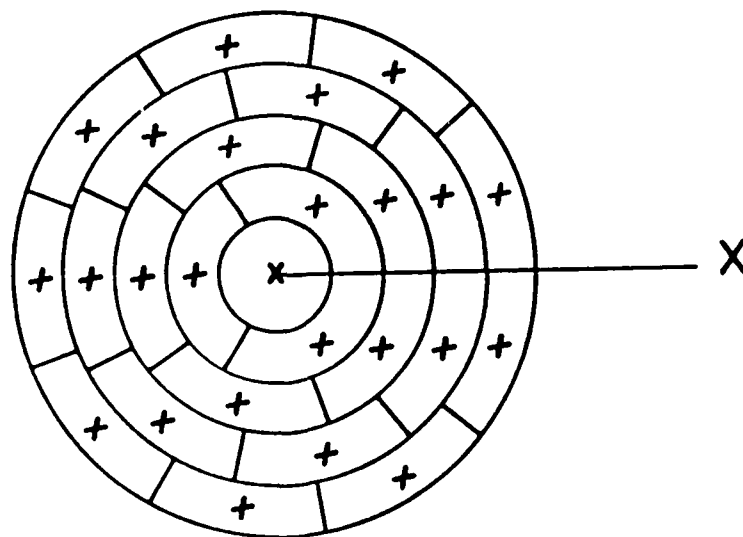


Figure 2. Division of the radius of the circular detector into 5 equal parts produces 5 annular rings (the 0th order ring is the central disc). Any n th order ring is subdivided into $(2n+1)$ equal elemental areas, the total number of which is 25. The central point of each of the elemental areas is marked by an "X".

three axis stabilized spacecraft) the telescope tilt angles with respect to the orbital plane. An example of this projection is shown in Figure 3.

To determine the relative efficiency, we need to find the portion of the cones in common as illustrated in Figure 4. This is done by first finding the maximum and minimum amounts of overlap which are possible, which determines the maximum and minimum pitch angles possible for the given point, and then iterating using a computer search algorithm to find the intersections for each pitch angle between the minimum and maximum. Once the points of intersection of the two cones are found, the fraction of overlap between the two cones, i.e. the efficiency, is determined.

The procedure is as follows. For a given point on the orbit, the calculation is performed at the center of the detector. Next a different sub-area is selected, and the calculation is repeated. This is continued until all of the elemental sub-areas of the detector have been completed. The results are then summed to give the efficiency for the whole detector. Then another point on the orbit is selected and the process repeated. In this way the efficiency as a function of pitch angle can be traced for all or any part of the satellite's orbit.

These calculations were checked against specific cases for which a complete analytic calculation could be done and were found to be in good agreement. In addition, checks were run that varied the step size in the search routine and the spacing of the grids in pitch angle, latitude and longitude. Finally, the detector area division was checked by using increased numbers of elemental sub-areas, up to $N = 10,000$. It was found that for $N > 100$, the results did not change appreciably.

The dependence of the efficiency on the parameters was studied first in a dipole model for the geomagnetic field. Figure 5 illustrates the variation in the efficiency function with latitude (λ), orbital inclination (ψ) and telescope tilt angle (δ). The notable points are the occurrence of the efficiency peak at a pitch angle $\alpha = 90^\circ$ for $\lambda = 0^\circ$ and $\psi = 90^\circ$, a shift in the peak pitch angle by $\sim 9^\circ$ for each 5° shift in latitude and the asymmetric nature of the efficiency curves away from $\lambda = 0^\circ$. The effect of the telescope tilt is to displace the curve to the right by $\sim 1^\circ$ in pitch angle per $\sim 3^\circ$ in tilt angle. Over the small range of ψ and δ investigated, there is little effect on the efficiency. Figure 6 shows the efficiency variation for $\alpha = 90^\circ$ particles as a function of latitude for three different telescope tilt angles. Again, there is little effect from the telescope tilt, but Fig. 6 also shows that 90° pitch angle particles are only observed effectively near the dipole equator.

For the real geomagnetic field we have used the IGRF75 model extended to 1982. The efficiency was first calculated at 10° intervals in geomagnetic longitude (ϕ) along the line of minimum magnetic field strength. On the average, the peak efficiency occurred at $\alpha = 88^\circ$ rather than $\alpha = 90^\circ$ as shown in Fig. 5 for the dipole approximation. Such a small difference allows us to use the dipole equator efficiency for the B_{\min} equator.

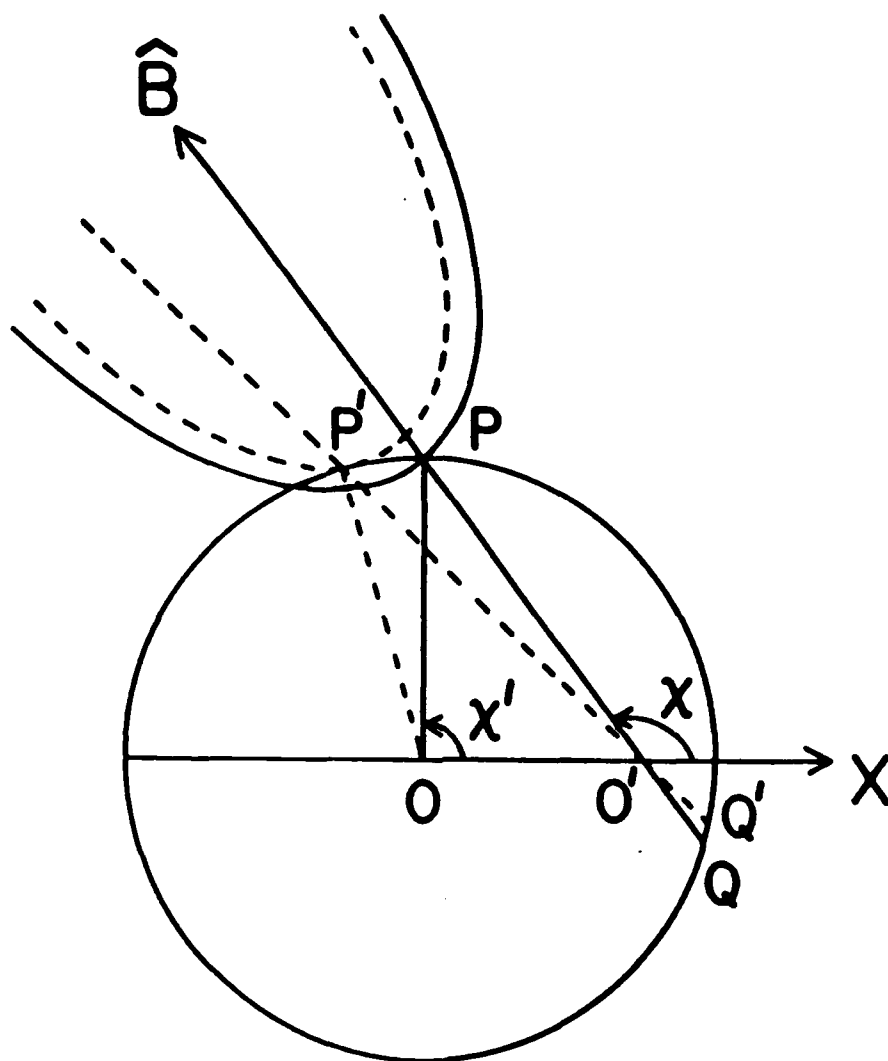


Figure 3. The circle is the opening ring of the detector. O' is the projection of the detector point $(a,0)$ under consideration. If the telescope cone is right circular, $QO'P$ is the projection of B , and the solid conic section is part of the projection of the pitch angle cone opening in the plane of the telescope opening ring. Points P and Q are the contact points for the minimum and the maximum pitch angle cones. If the telescope cone is simply circular, the dotted line and the dotted conic section become the projections, and P' and Q' become the contact points.

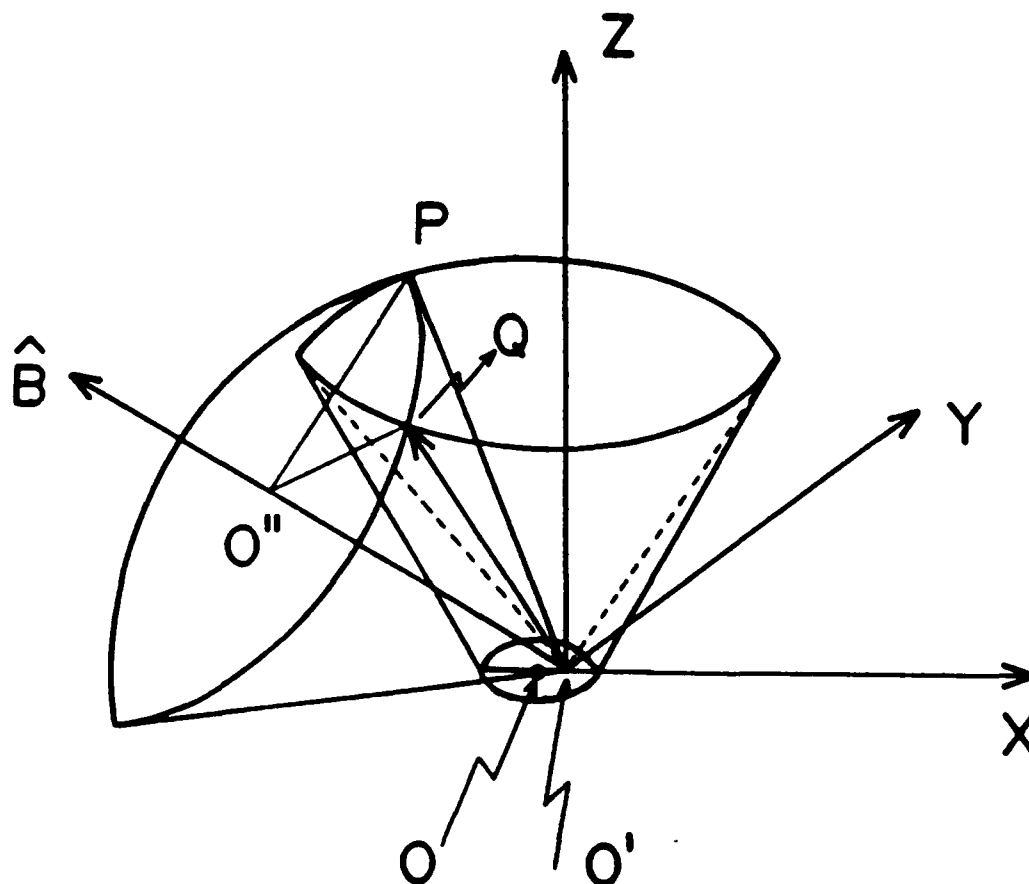


Figure 4 The point O' is at $(a,0)$ on the detector. $O'Z$ and $O'O''$ are the axes of the telescope and the pitch angle cones, respectively, P and Q are the points of intersection of the two cones. The part $O'O''PQ$ of the whole pitch angle cone is intercepted by the telescope cone.

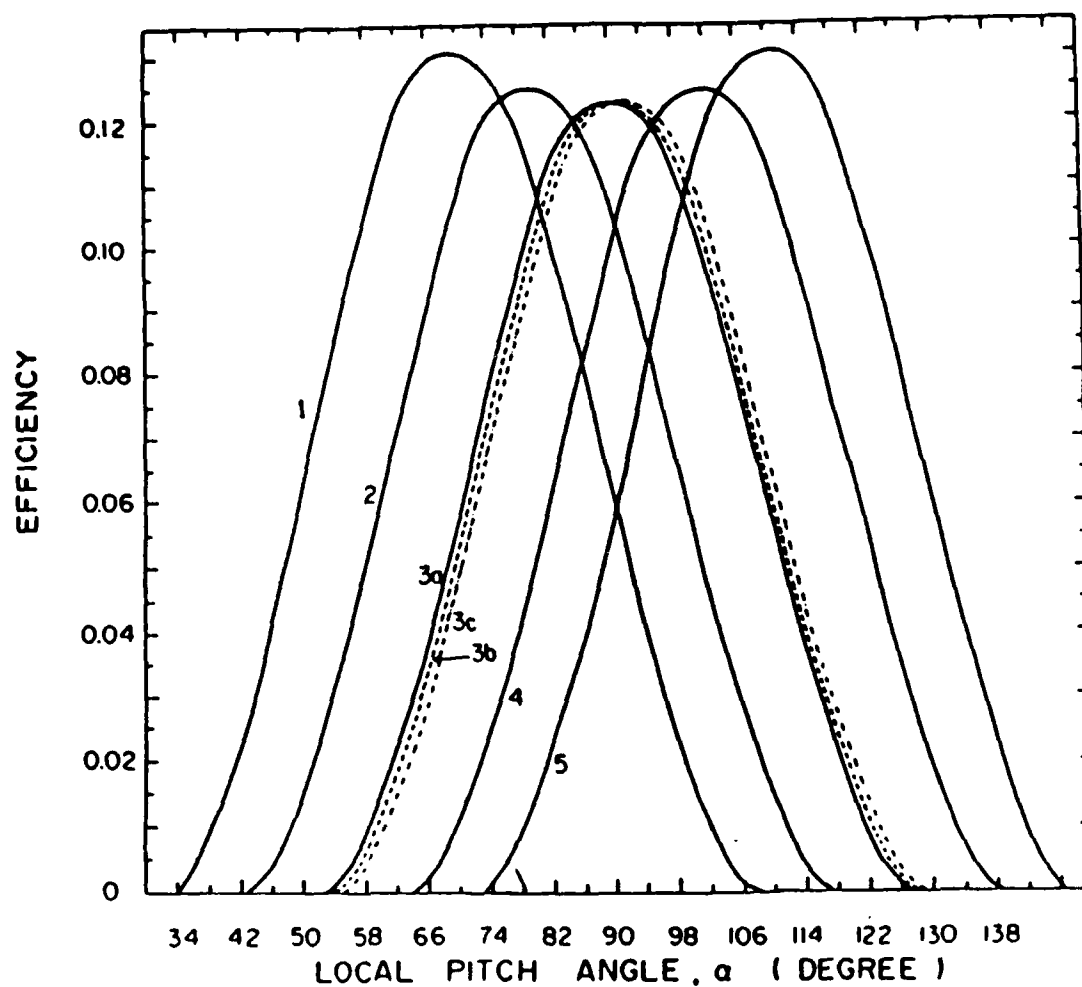


Figure 5 Latitude and tilt angle variation of efficiency. Curves 1, 2, 3a, 4, and 5 are drawn at $\lambda = 10^\circ, 5^\circ, 0^\circ, -5^\circ, -10^\circ$ respectively, for $\psi = 90^\circ$ and $\delta = 2.35^\circ$. $\delta = 2.35^\circ$ and $\psi = 110^\circ$ for curve 3b; $\delta = 5.0^\circ$ and $\psi = 110^\circ$ for curve 3c.

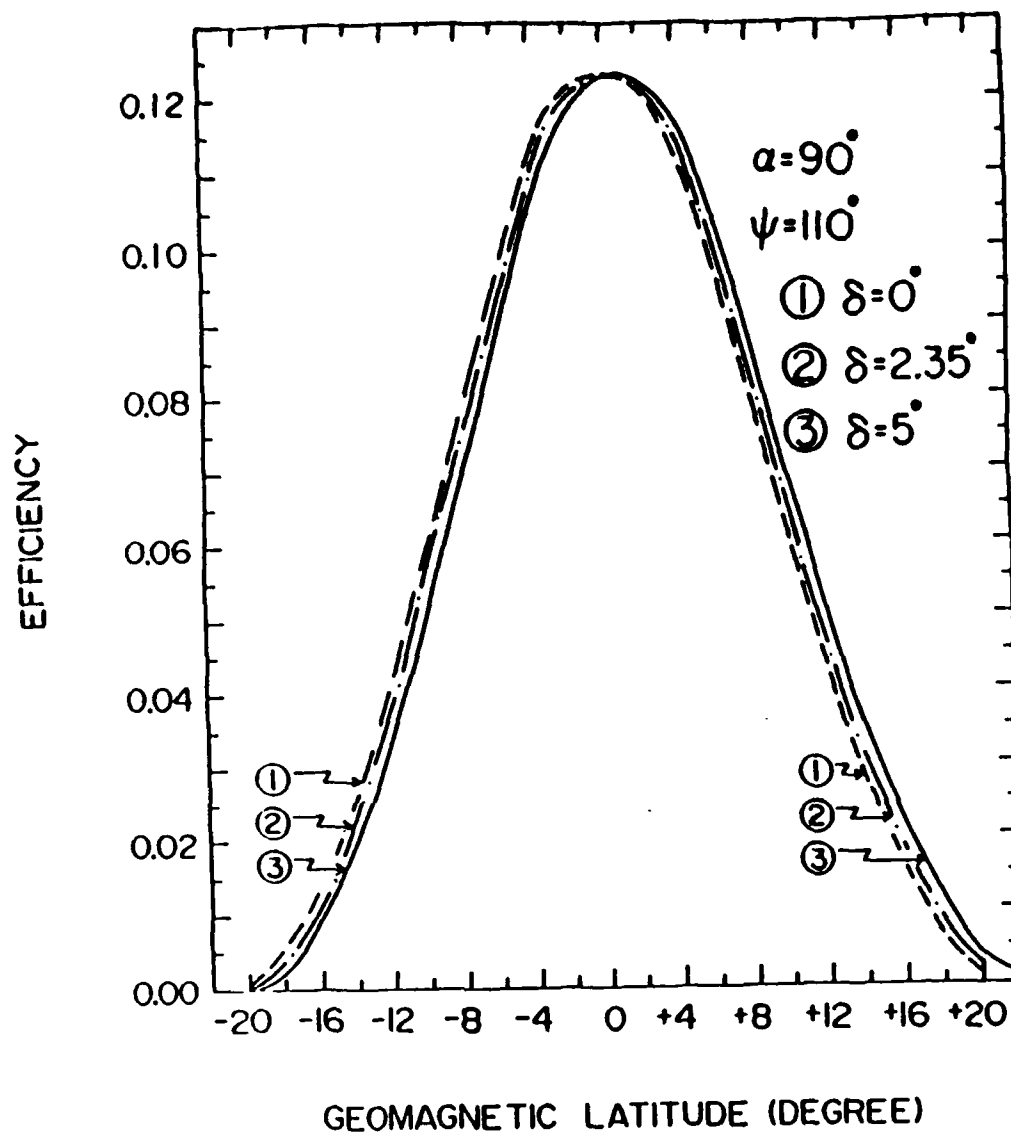


Figure 6. Variation of efficiency for mirroring particles with the angle of tilt. All of the curves have the same $\psi = 110^\circ$. The curves shift to the right with increasing δ .

Unlike the dipole field, however, in the real field the efficiency is a function of longitude, as shown in Fig. 7. Neither the efficiency function evaluated at equal intervals on either side of the B_{\min} equator and at the same longitude, nor the efficiency function evaluated at the same interval on the same side of the B_{\min} equator and at different longitudes, are in agreement. The efficiency varies by 5% to 30% within $\pm 10^\circ$ in latitude from minimum B latitudes. Thus, at off- B_{\min} points in the real field, the efficiency function deviates from the values at equivalent points in the dipole field. Finally, the efficiency was found to vary little with altitude (over a 500 km altitude change, the efficiency curve shifts by a maximum of $\sim 2^\circ$ in pitch angle).

The efficiency function can now be used to determine the actual intensity of the ~ 1 MeV protons observed by ONR-602 in 1982 and to compare these observations to those made about a decade earlier. To do this it is necessary to evaluate the efficiency function for the smaller telescope used by Moritz on the Azur satellite. This was done with the same technique described above using published values the parameters applicable to the Azur instrument. Figure 8 shows the comparison. The Azur telescope had a much narrower opening cone and therefore responded to particles closer to 90° in pitch angle. The Azur telescope also had a smaller detector, and this difference must be included in calculating the intensity.

In both cases we begin with the peak particle counting rate observed. For Azur, the energy interval is smaller than it was for Phoenix-1 so the observed rate was increased, using the spectrum reported from Azur, to obtain the counting rate that would have been observed over the full energy interval. The efficiency function is then folded with an assumed pitch angle distribution, in the range obtained for Azur measurements, and the intensity adjusted to reproduce the observed counting rate. Figure 9 shows the result as a function of the index of the assumed pitch angle distribution. Note that there is little sensitivity to q for $q > 7$, the range relevant to these quasi-trapped particles. Our measurements at an altitude of 277 km are in agreement with the previous data at 450 km altitude. However, when our data is extrapolated, using the measured altitude dependence, to an equal altitude (450 km), we find almost an order-of-magnitude larger flux in 1982 compared to 1969-1970. This is evidence for a long term temporal variation in this population, due either to an enhanced source, e.g. the ring current, or to differing atmospheric conditions which affect the production and loss of these quasi-trapped particles.

Another possible source of variation may be the solar conditions applicable to the two epochs. Figure 10 shows several solar activity monitors for the period 1965-1984. Comparison shows that the solar activity levels in 1982 were very similar to those in 1969-1970, and the mean atmospheric density shows only a small increase in 1982 over the earlier period. Such a small increase is probably insufficient to explain the enhanced particle intensity.

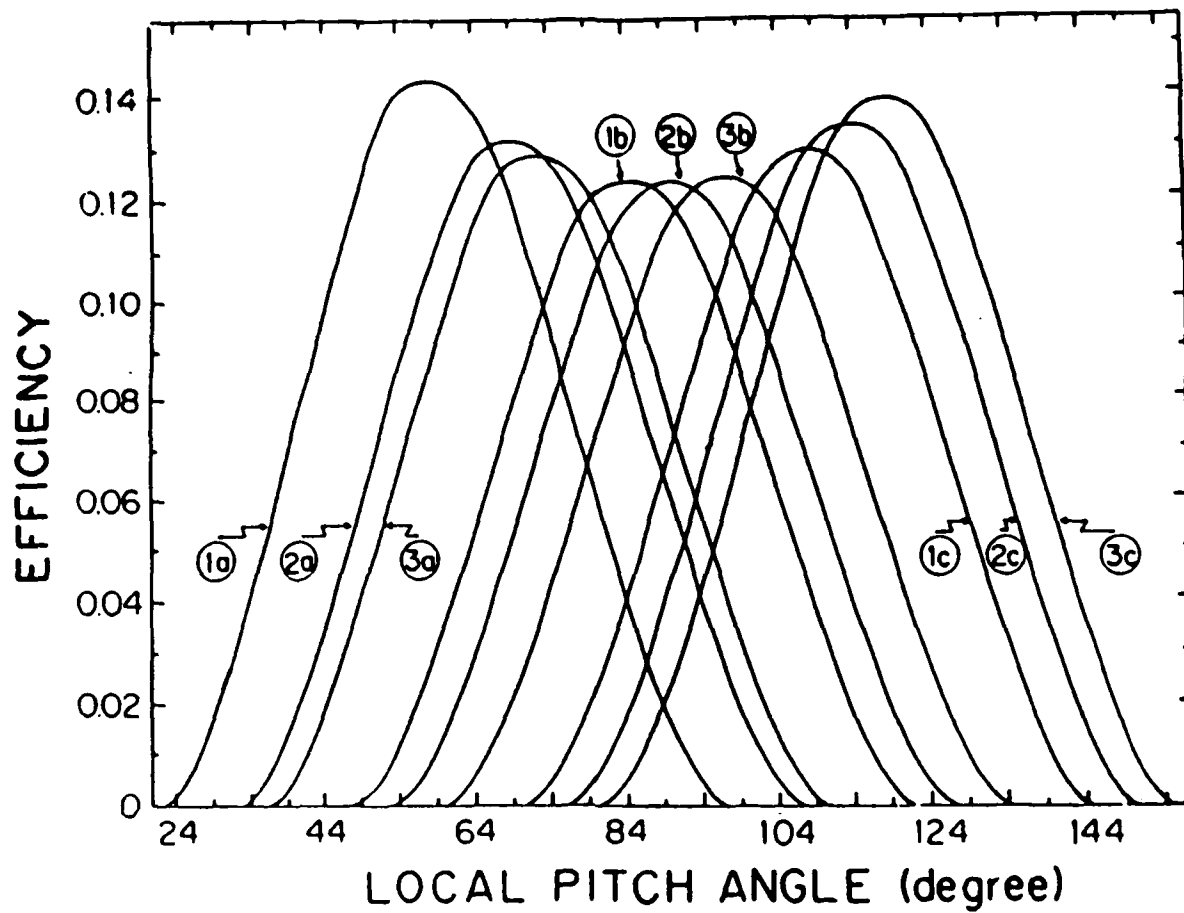


Figure 7. Variation of efficiency function in the real field as a function of latitude and longitude. b-curves are at latitudes of the minimum \tilde{B} equator. a-curves are -10° , and c-curves are $+10^\circ$ away from the latitudes of minimum \tilde{B} . Curves (1a, 1b, 1c) are at $\phi = 102^\circ$, (2a, 2b, 2c) are at $\phi = 270^\circ$, and (3a, 3b, 3c) are at $\phi = 230^\circ$. $\delta = 2.35^\circ$ and $\psi = 90^\circ$ for all curves.

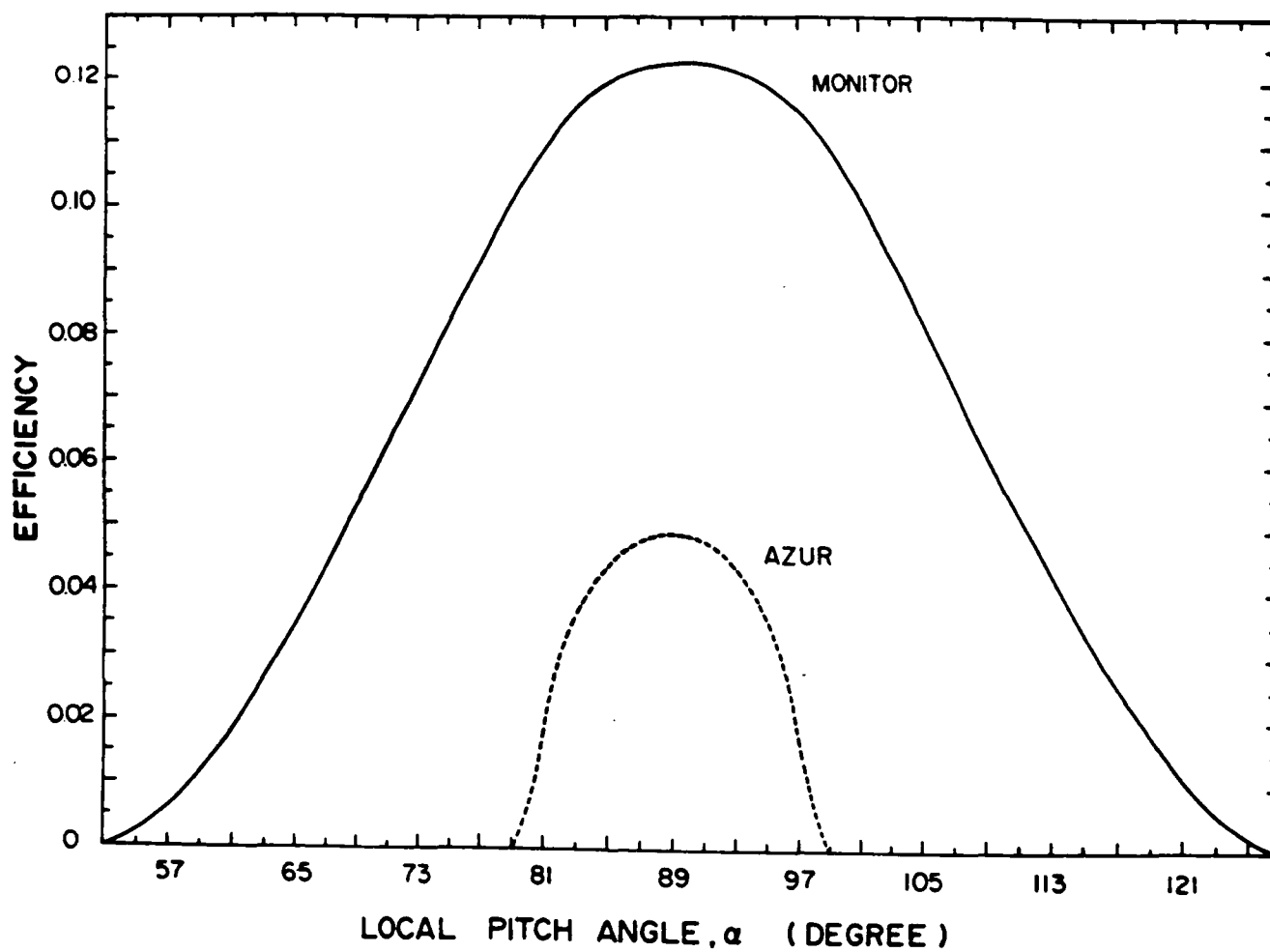


Figure 8. Comparison of the efficiency function calculated for the Phoenix-1 monitor telescope with an identical calculation for the telescope on the Azur satellite used by Moritz.

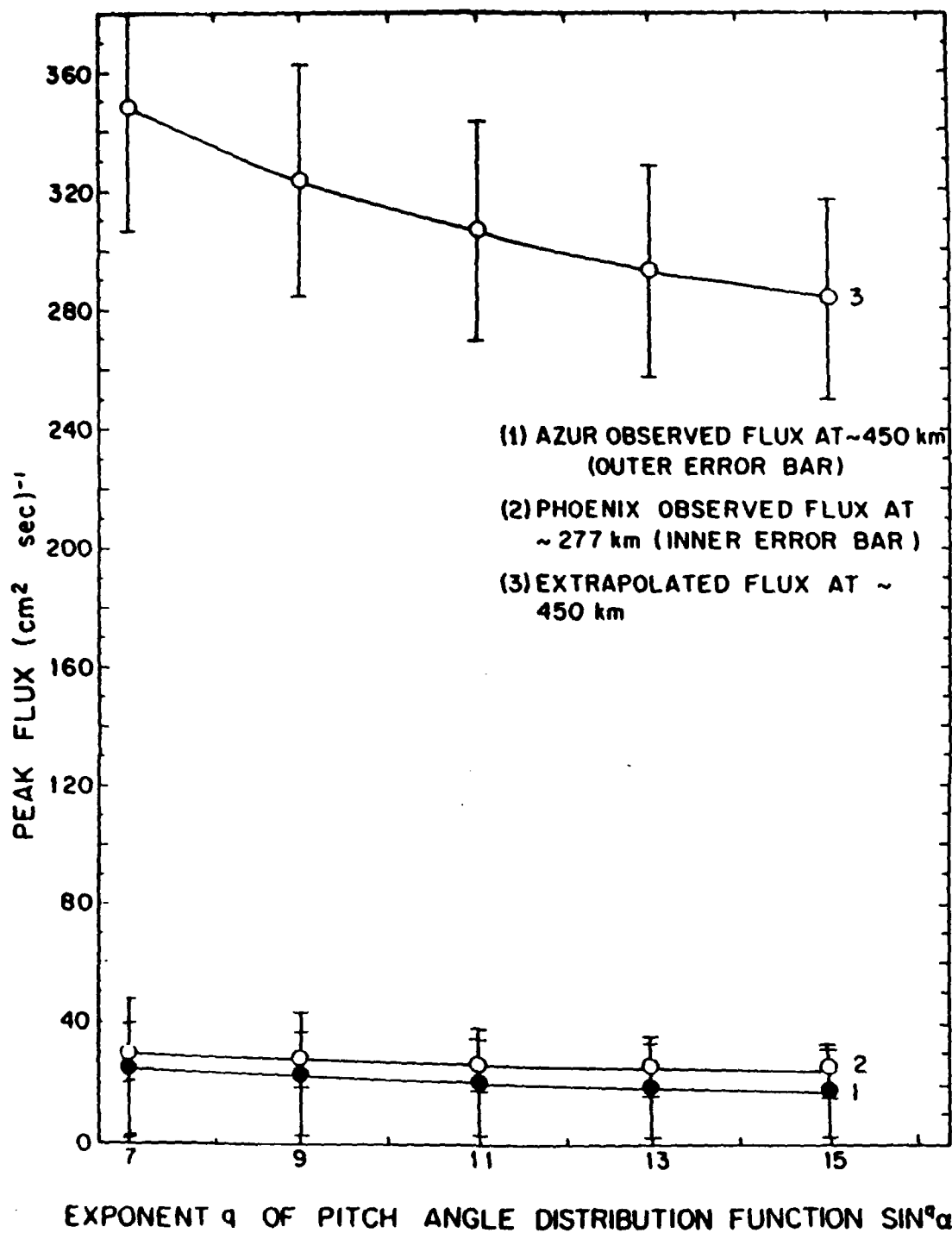


Figure 9. Comparison of the intensity, calculated from the peak counting rate, for the Phoenix-1 and the Azur instruments. Results from Phoenix-1 are given at the observation altitude of 277 km and extrapolated to 450km, the altitude of the Azur observations.

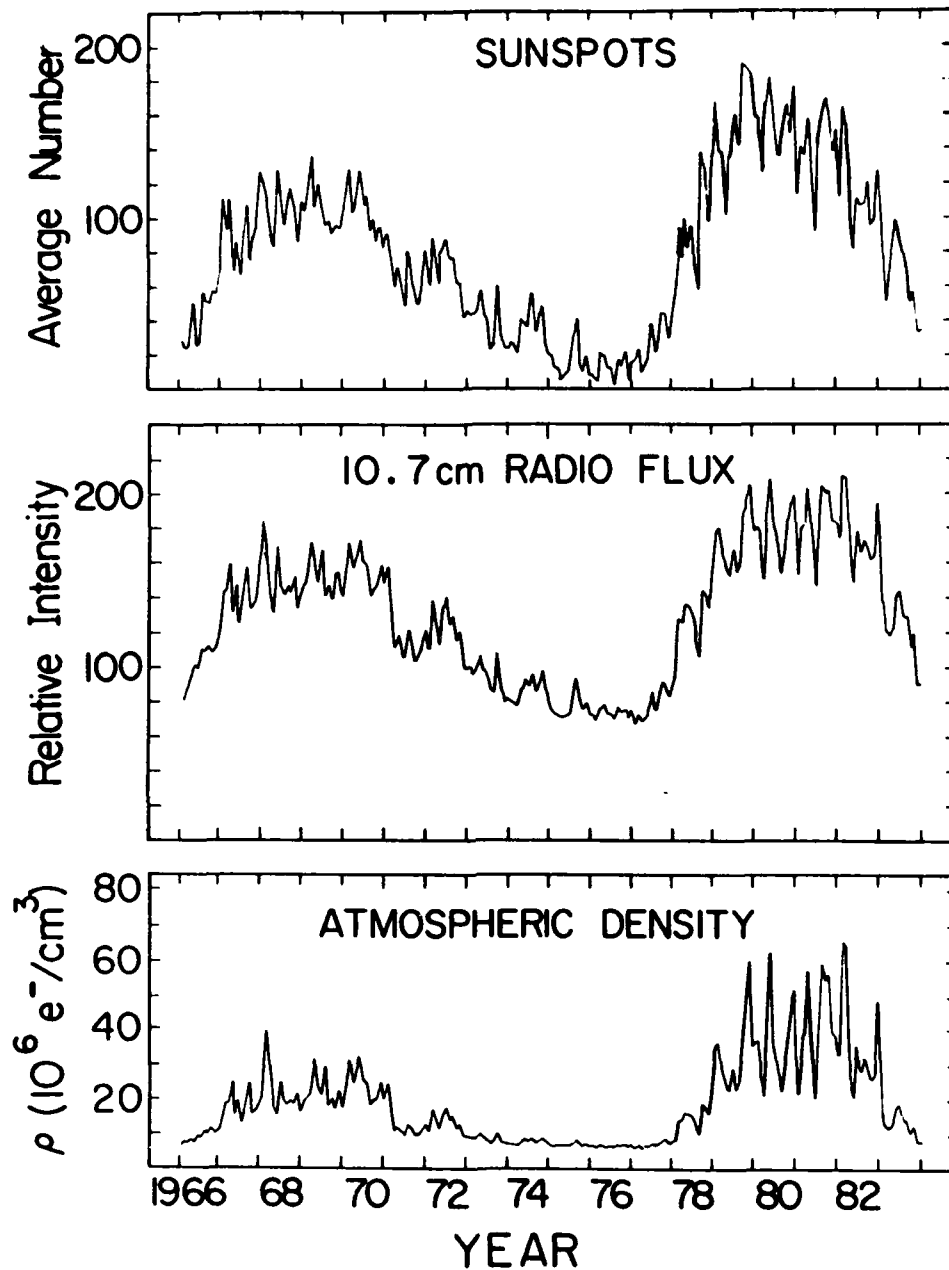


Figure 10. Solar Activity Indicators for 1966-1984. Note that the levels for 1969-1970 and for the last half of 1982 are very similar.

VI. Research Plans:

What is still needed for a detailed understanding of the low energy proton component observed by Phoenix-1 is a complete model of the particle precipitation process. Such a model does not exist in the literature, and the potential importance of this component, both as a tracer of processes occurring high in the magnetosphere and as a radiation background for missions in LEO, requires such a model. Thus, a major thrust of our work for the coming year will be to develop a detailed model of the physical processes affecting this radiation. This model must be capable of explaining the measured altitude dependence, the flux profile, the lack of a longitude dependence and the intensity variations observed in the data.

In addition to the model development, we will continue our analysis of other regions of the S81-1 orbit, particularly the work begun on the South Atlantic Anomaly, and will refine the solar flare database for additional flare investigations. Some portion of our effort in the coming year will also be devoted to beginning the ONR-604 pre-launch preparations and science planning.

Late Abstracts

(No. 2)

**Chapman Conference on
Plasma Waves and Instabilities
in Magnetospheres and at Comets**



**October 12-16, 1987
Sendai/Mt. Zao, Japan
Convenors: Hiroshi Oya and Bruce T. Tsurutani**

(Oct. 11 : Reception and Registration)

LOW ENERGY PROTONS

AT THE EQUATOR

M. A. Miah, J. W. Mitchell, T. G. Guzik and J. P. Wefel

Department of Physics and Astronomy
Louisiana State University
Baton Rouge, LA 70803-4001

ABSTRACT

Magnetospheric particles, trapped in the radiation belts, are lost at low altitudes and precipitated into the atmosphere all over the globe. Based upon observations of low energy (keV) ions and electrons as summarized by Voss and Smith (1980) the different global zones of particle precipitation are: (1) the equatorial zone, (2) the low-latitude zone, (3) the mid-latitude zone, and (4) the auroral zone. In the equatorial zone, which is investigated in this paper, protons are the principal ionic component and the mechanism responsible for the low altitude proton flux seems to be charge exchange of the outerbelt protons with the thermal neutral hydrogen atoms of the exosphere according to the reaction: $P^+ + H \rightarrow H^+ + P$, where a $^+$ indicates an energetic component. The neutrals leave the source region in a direction which depends upon the proton's velocity vector at the time of neutralization. A fraction of these neutrals are directed toward the Earth and, at low altitude, the neutrals are stripped of their electrons by collisions with the atmosphere. The ions so generated become trapped, temporarily, in the Earth's magnetic field forming a low altitude "belt". These quasi-trapped protons may undergo additional cycles of electron capture and stripping before finally being lost into the atmosphere. It takes about 7 such cycles for vertically traveling neutrals of ~ 1 MeV and 90° equatorial pitch angle to move from 1000 km to 160 km altitude.

Our investigation of the equatorial particle precipitation was performed with the Phoenix-1 instrument on board the S81-1 mission from May through November, 1982. The satellite was in a low altitude ($\sim 170 - 290$ km) nearly circular polar orbit, inclination ~ 85 degrees, with an orbital plane from 10:30 - 22:30 local time, and a period of ~ 90 minutes. The Phoenix-1 instrument included two telescopes: the monitor telescope and the main telescope. The main telescope was used to determine the charge and mass of solar energetic particles with energies ≥ 10 MeV/nucleon, an energy threshold too high to observe the low energy precipitating protons. The data presented here are derived from the monitor telescope which is a passively shielded, single silicon detector (40μ thick) instrument with an opening angle of 75° and a geometrical factor of $\sim 0.5 \text{ cm}^2\text{-sr}$. designed to study low energy particles. This telescope returned three counting rates -- ML, MM, and MH -- corresponding to three different energy deposit thresholds. The ML threshold of 0.36 MeV records protons (0.6 - 9 MeV), alphas (0.4 - 80 MeV) and heavy ions. Rate MM responds to alphas (0.8 - 4.5 MeV) and heavy ions, while MH observes only heavy ions. The thin detector employed made the monitor insensitive to electrons and the passive shielding was sufficient to stop up to ~ 45 MeV protons incident outside the opening cone. For the equatorial zone, the MH rate was consistent with cosmic ray background and $\text{MH/ML} \sim 10^{-3}$ which indicates that protons are the dominant species.

Our analysis of the equatorial zone has focussed on the region -30° to $+30^\circ$ in geomagnetic latitude, and this band was binned in 1° (latitude) by 5° (longitude) bins. The average proton counting rate was determined in each bin and latitude plots were made for each longitude region. The locations (in latitude) of the peaks are shown in the top panel of Fig. 1. The bottom panel gives the location of the line of minimum magnetic field strength, B_{\min} (Stassinopoulos, 1970), and our measured proton flux maxima follow the line. This profile can be understood from the fact that protons trapped at low altitude in the equatorial region experience a harmonic bounce motion about the B_{\min} value of the geomagnetic field, which is also the position of minimum magnetic field energy density ($\approx 6.2 \times 10^{-5} \text{ B}^2/8\pi \text{ MeV-cm}^{-3}$). The latitude width of the equatorial zone, determined from a superposition of all passes, was 10° (FMM).

The altitude range sampled by the spacecraft was divided into 5 - 15 km wide bands so as to keep comparable numbers of passes in each altitude range. All passes whose peak values occurred in a given altitude band were superposed, peak-to-peak, to determine the average peak flux. Figure 2 shows a plot of the relative

flux versus altitude. The flux follows a power law in altitude, and a fit to the data yields an exponent of 5.0 ± 0.2 . As indicated on the figure, the slope of our data correlates well with that of Filz and Holeman (1965) who, from the correlation of their results with the reciprocal of average atmospheric density, confirmed that the 55 MeV protons are lost through atmospheric ionization. Whereas 55 MeV protons can be lost only through energy loss in the atmosphere, the protons observed in the Phoenix-1 instrument can be lost both by electron capture and by atmospheric ionization. An investigation is underway to assess the contribution of each process, integrated over the energy and the pitch angle ranges of the instrument, as a function of altitude in order to understand quantitatively the measured altitude dependence of the proton flux.

Figure 3 shows the peak differential flux observed in 1982 compared to that measured by previous missions (Moritz, 1972; Hovestadt et al., 1972; Mizera and Blake, 1973), during both geomagnetic storm and quiet times. The storm time inflation is pronounced for the lower energy protons but is not observed above $\sim 0.5 \text{ MeV}$. For the prestorm or average data above 100 keV, a least square fit to a power-law is shown by the solid line for $J(E) = b E^{-k}$ with $b = 6 \times 10^5/\text{cm}^2\text{-sr-s-keV}^{-k}$ and $k = 2.55 \pm 0.11$. From this fit the mean energy of the protons observed by the monitor telescope is $\sim 1.3 \text{ MeV}$, and we would expect to observe a flux of $\sim 19 \text{ cm}^{-2} \text{ s}^{-1} \text{ sr}^{-1}$.

The highest altitude bin in the analysis was centered at 277 km, whereas the lowest observation altitude of previous missions was $\sim 450 \text{ km}$. To compare

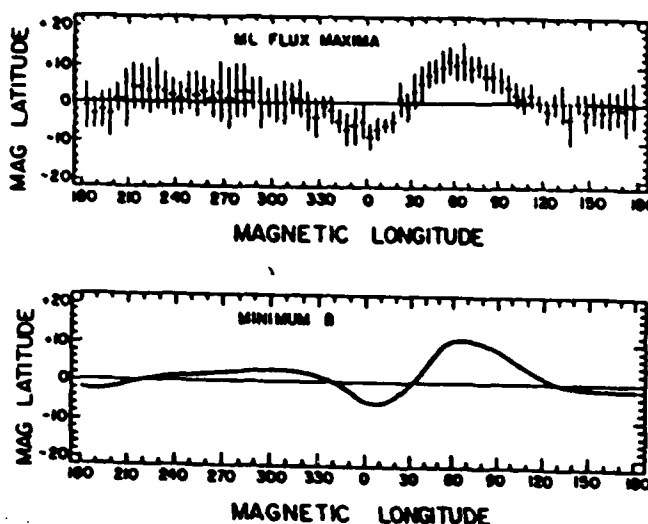


Figure 1. Global profile of maximum proton flux.

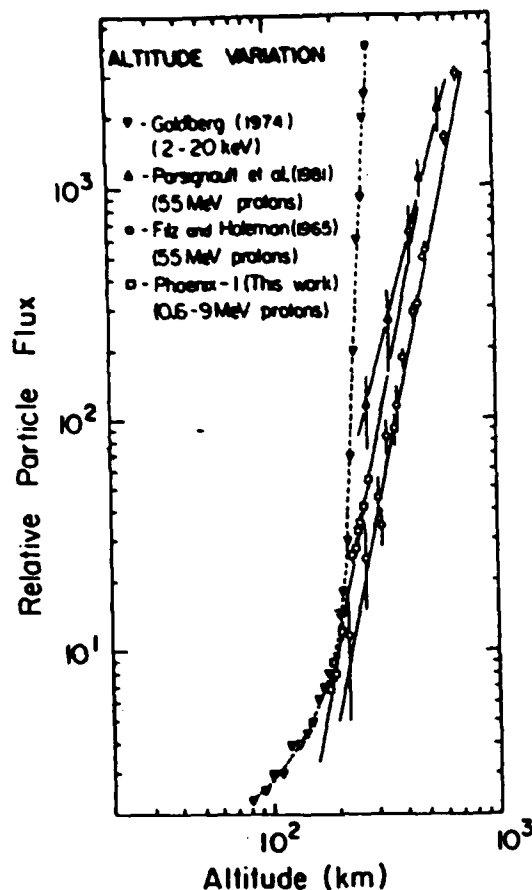


Figure 2. Altitude Dependence

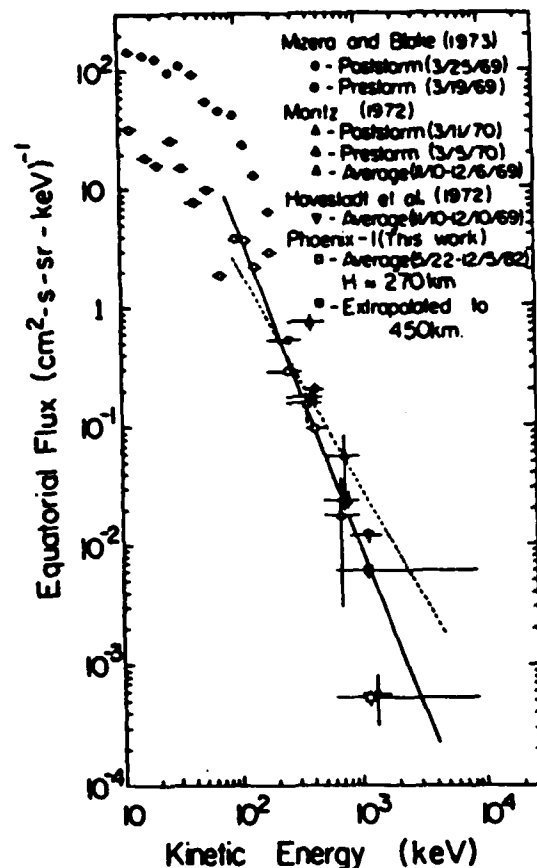


Figure 3. Differential Energy Spectrum

the observed flux with previous missions, we extrapolated to 450 km using the altitude dependence derived from Fig. 2. This gives a flux of $53 \text{ cm}^{-2} \text{ s}^{-1} \text{ sr}^{-1}$ which is a factor of 2.8 larger than that expected from the power law fit on Fig. 3. To reproduce our extrapolated flux and the previous values at 100 - 200 keV would require a power law spectrum such as is indicated by the dashed line on the figure, and this line clearly does not fit most of the previous measurements.

An increased proton flux at low altitudes in 1982 compared to measurements made ~1970 could signal a temporal change in the outer belt particle population and/or an increase in the exospheric hydrogen density, possibly due to differing solar conditions. However, some of the difference may be due to the assumption of omni-directional particles which was employed in the scaling for telescope solid angle. Such an assumption neglects the actual pitch angle distribution of the particles which Mizra and Blake (1973) found to have a dependence of approximately $(\sin \alpha)^{-10}$. The larger acceptance range of the Phoenix-1 instrument compared to the previous instruments may account for some of the difference in observed flux. In progress is a calculation of detector efficiency as a function of equatorial pitch angle, and geomagnetic latitude and longitude, including the orbital inclination and the tilt of the telescope

axis. This will allow a better determination of the proton flux and energy spectrum which can then be compared, in detail, to the charge exchange model for the origin of these particles.

ACKNOWLEDGEMENT

The work was supported by ONR Contract N-00014-83-K-0365.

REFERENCES

- Filz, R. C. and Holeman, E., 1965, J. Geophys. Res., 70, 5807.
Goldberg, R. A., 1974, J. Geophys. Res., 79, 5299.
Hovestadt, D., Hausler, B., and Scholer, M., 1972, Phys. Rev. Lett., 28, 1340.
Mizera, P. F. and Blake, J. B., 1973, J. Geophys. Res., 78, 1058.
Moritz, J., 1972, Z. Geophys., 38, 701.
Parsignault, D. R. and Holeman, E., 1981, J. Geophys. Res., 86, 11439.
Spjeldvik, W. N. and Fritz, T. A., 1983, in Energetic Ion Composition in the Earth's Magnetosphere, ed. R. G. Johnson, p. 396, D. Reidel Publishing Co., Dordrecht.
Stassinopoulos, E. G., 1970, World Maps of Constant B, L and Flux Contours, NASA SP-3054, Goddard Space Flight Center, Greenbelt, MD, p. 58.
Voss, H. D. and Smith, L. G., 1980, J. Atmos. Terr. Phys., 42, 227.

END

DATE

FILM

DTIC

7-85